

REPORT DOCUMENTATION PAGE				Form Approved OMB No. 0704-0188	
Public reporting burden for this collection of information is estimated to average 1 hour per response, including the time for reviewing instructions, searching existing data sources, gathering and maintaining the data needed, and completing and reviewing this collection of information. Send comments regarding this burden estimate or any other aspect of this collection of information, including suggestions for reducing this burden to Department of Defense, Washington Headquarters Services, Directorate for Information Operations and Reports (0704-0188), 1215 Jefferson Davis Highway, Suite 1204, Arlington, VA 22202-4302. Respondents should be aware that notwithstanding any other provision of law, no person shall be subject to any penalty for failing to comply with a collection of information if it does not display a currently valid OMB control number. PLEASE DO NOT RETURN YOUR FORM TO THE ABOVE ADDRESS.					
1. REPORT DATE (DD-MM-YYYY) 23-11-2009		2. REPORT TYPE Journal Article		3. DATES COVERED (From - To)	
4. TITLE AND SUBTITLE Synthesis and Properties of N ₇ O ⁺ (PREPRINT)				5a. CONTRACT NUMBER	
				5b. GRANT NUMBER	
				5c. PROGRAM ELEMENT NUMBER	
6. AUTHOR(S) Karl O. Christe, Ralf Haiges, and William W. Wilson (USC); Jerry A. Boatz(AFRL/RZSP)				5d. PROJECT NUMBER	
				5e. TASK NUMBER	
				5f. WORK UNIT NUMBER 50260541	
7. PERFORMING ORGANIZATION NAME(S) AND ADDRESS(ES) Air Force Research Laboratory (AFMC) AFRL/RZSP 10 E. Saturn Blvd. Edwards AFB CA 93524-7680				8. PERFORMING ORGANIZATION REPORT NUMBER AFRL-RZ-ED-JA-2009-413	
9. SPONSORING / MONITORING AGENCY NAME(S) AND ADDRESS(ES) Air Force Research Laboratory (AFMC) AFRL/RZS 5 Pollux Drive Edwards AFB CA 93524-7048				10. SPONSOR/MONITOR'S ACRONYM(S)	
				11. SPONSOR/MONITOR'S NUMBER(S) AFRL-RZ-ED-JA-2009-413	
12. DISTRIBUTION / AVAILABILITY STATEMENT Approved for public release; distribution unlimited (PA #09507).					
13. SUPPLEMENTARY NOTES For the Journal of Inorganic Chemistry					
14. ABSTRACT The reaction of NOF ₂ +SbF ₆ ⁻ with an equimolar amount of HN ₃ in anhydrous HF solution at -45 °C produces N ₃ NOF+SbF ₆ ⁻ . When an excess of HN ₃ is used in this reaction, N ₇ O+SbF ₆ ⁻ is formed. However, this compound could not be isolated as a solid and rapidly decomposed in a quantitative manner with N ₂ O evolution to N ₅ +SbF ₆ ⁻ . This reaction represents a novel and more convenient synthesis for N ₅ +SbF ₆ ⁻ because NOF ₂ +SbF ₆ ⁻ is more readily accessible than N ₂ F+SbF ₆ ⁻ and the N ₅ ⁺ can be labeled in all five positions with ¹⁵ N by the simple use of terminally singly-labeled N ₃ ⁻ . The formation of the N ₇ O ⁺ cation was established by isotopic labeling experiments and theoretical calculations. It is shown that the addition of a second azido ligand to the same central atom allows attack of the negatively charged N α atom of one ligand by the positively charged N γ atom of the second ligand, thereby greatly lowering the activation energy barrier towards decomposition and explaining why geminal di-azides are much less stable than either mono-azides or vicinal di-azides. Keywords: polynitrogen chemistry, heptanitrogen oxide cation, theoretical calculations, activation energy barriers.					
15. SUBJECT TERMS					
16. SECURITY CLASSIFICATION OF:			17. LIMITATION OF ABSTRACT SAR	18. NUMBER OF PAGES 20	19a. NAME OF RESPONSIBLE PERSON Wayne Kallioma
a. REPORT Unclassified	b. ABSTRACT Unclassified	c. THIS PAGE Unclassified			19b. TELEPHONE NUMBER (include area code) N/A

Synthesis and Properties of N_7O^+ (PREPRINT)

Karl O. Christe^{†}, Ralf Haiges[†], William W. Wilson[†] and Jerry A Boatz[‡]*

[†]Loker Research Institute and Department of Chemistry, University of Southern California, Los Angeles, CA 90089-1661, USA, and [‡]Air Force Research Laboratory, Edwards Air Force Base, CA, 93524 USA.

* To whom correspondence should be addressed: E-mail: kchriste@usc.edu

RECEIVED DATE _____

Synthesis and Properties of N_7O^+

Author to whom correspondence should be addressed. E-mail: kchriste@usc.edu.

ABSTRACT: The reaction of $\text{NOF}_2^+\text{SbF}_6^-$ with an equimolar amount of HN_3 in anhydrous HF solution at $-45\text{ }^\circ\text{C}$ produces $\text{N}_3\text{NOF}^+\text{SbF}_6^-$. When an excess of HN_3 is used in this reaction, $\text{N}_7\text{O}^+\text{SbF}_6^-$ is formed. However, this compound could not be isolated as a solid and rapidly decomposed in a quantitative manner with N_2O evolution to $\text{N}_5^+\text{SbF}_6^-$. This reaction represents a novel and more convenient synthesis for $\text{N}_5^+\text{SbF}_6^-$ because $\text{NOF}_2^+\text{SbF}_6^-$ is more readily accessible than $\text{N}_2\text{F}^+\text{SbF}_6^-$ and the N_5^+ can be labeled in all five positions with ^{15}N by the simple use of terminally singly-labeled N_3^- . The formation of the N_7O^+ cation was established by isotopic labeling experiments and theoretical calculations. It is shown that the addition of a second azido ligand to the same central atom allows attack of the negatively charged N α atom of one ligand by the positively charged N γ atom of the second ligand, thereby greatly lowering the activation energy barrier towards decomposition and explaining why geminal di-azides are much less stable than either mono-azides or vicinal di-azides.

Keywords: polynitrogen chemistry, heptanitrogen oxide cation, theoretical calculations, activation energy barriers.

Introduction

An area of particular interest for energetic materials is high-nitrogen chemistry. In high-nitrogen chemistry most of the energy release stems from the fact that N-N single bonds (average bond energy ~159 kJ/mol) and N=N double bonds (average bond energy ~419 kJ/mol) are considerably weaker than one third or two thirds of the N≡N triple bond energy in dinitrogen (bond energy of 946 kJ/mol). Therefore, polynitrogen compounds possess large positive heats of formation and decompose exothermically with the liberation of large amounts of N₂. The formation of large amounts of N₂ in the decomposition products is highly desirable for applications such as gun propellants where the smoke, flame temperature and the corrosion of the gun barrels are greatly reduced by the N₂. During the last decade, major breakthroughs in this field have been achieved by the syntheses and identification of several novel ions, the V-shaped N₅⁺ cation,^{1,2} the N₃NOF⁺ cation both as a *z*- and *e*-isomer,³ and the *cyclo*-N₅⁻ anion.⁴ The chemistry of N₅⁺ and N₅⁻ has been highlighted in a recent review paper.⁵ The synthesis and characterization of N₃NOF⁺ has also been described already in detail,³ and here the synthesis of the N₇O⁺ cation is reported. In particular, the question of why N₇O⁺ is thermally so much less stable than N₃NOF⁺ is addressed, and whether this instability is innate to geminal di-azides.

Experimental Section

Caution! Neat HN₃ is highly explosive and should, whenever possible, be handled only in solution. Anhydrous HF can cause severe burns and contact with the skin must be avoided.

Materials and Apparatus: All reactions were carried out in Teflon-FEP ampules that were closed by stainless steel valves. Volatile materials were handled in a stainless steel/Teflon-FEP vacuum line.⁶ All reaction vessels and the vacuum line were passivated with ClF₃ prior to use. Nonvolatile materials were handled in the dry argon atmosphere of a glove box.

Raman spectra were recorded in the Teflon reactors in the range 4000–80 cm⁻¹ on a Bruker Equinox 55 FT-RA spectrophotometer, using a Nd-YAG laser at 1064 nm or a Cary Model 83GT spectrometer

using the 488-nm line of an Ar-ion laser. The ^{14}N NMR spectra were recorded in anhydrous HF as solvent on a Bruker AMX-500 NMR instrument at 36.13 MHz using a 5 mm broad band probe. Neat CH_3NO_2 ($\delta = 0$ ppm), measured at room temperature, was used as an external standard.

The starting materials, $\text{NOF}_2^+\text{SbF}_6^-$ ⁷ and HN_3 ² were prepared by literature methods. HF was dried by storage over BiF_5 ⁸ or TaF_5 .

Reaction of $\text{NOF}_2^+\text{SbF}_6^-$ with HN_3 : In a typical experiment, $\text{NOF}_2^+\text{SbF}_6^-$ (0.3 mmol) was added to a pre-passivated, thin-walled, 4 mm o.d. FEP ampule, which was closed by a stainless steel valve. On the vacuum line, anhydrous HF (270 mg) was condensed in at $-196\text{ }^\circ\text{C}$ and the $\text{NF}_2\text{O}^+\text{SbF}_6^-$ was dissolved in the HF at room temperature. The ampule was cooled back to $-196\text{ }^\circ\text{C}$, and a mixture of HN_3 (0.3 or 0.6 mmol) and HF (750 or 1500 mg, respectively) was condensed in. The FEP ampule was heat sealed and warmed to $-80\text{ }^\circ\text{C}$. It was then inserted into a standard 5 mm o.d. glass NMR tube and quickly transferred into the probe of the NMR spectrometer. The sample was warmed to ambient temperature in steps of $10\text{ }^\circ\text{C}$ and monitored by NMR spectroscopy.

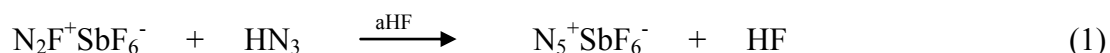
Theoretical Methods: The molecular structures, harmonic vibrational frequencies, and infrared and Raman vibrational intensities were calculated using (a) second order perturbation theory (MP2, also known as MBPT(2)⁹) and the 6-311G(2df) basis set,¹⁰ denoted as MP2/6-311G(2df), (b) MP2 with the correlation consistent polarized valence triple-zeta basis set,¹¹ i.e., MP2/cc-pvtz, and (c) density functional theory methods using the B3LYP hybrid functional,¹² which included the VWN5 correlation functional¹³ and the 6-311G(2df) basis set (B3LYP/6-311G(2df)). In addition, the structure and harmonic vibrational frequencies of the C_{2v} isomer of N_7O^+ were computed using the coupled cluster singles plus doubles with a perturbative estimate of triples (CCSD(T)¹⁴) method, with the 6-31G(d) basis set.¹⁵ Hessians (energy second derivatives) were calculated for all stationary points to verify them as either local minima or transition states (i.e., having zero or one negative eigenvalue of the Hessian, respectively.) Intrinsic reaction coordinate¹⁶ traces were generated using the Gonzales-Schlegel second-order method.¹⁷ The relative energies of all stationary points were refined by performing “completely renormalized” CR-CCSD(T)¹⁸ single point energy computations at the MP2/6-311G(2df) geometries.

B3LYP/6-311G(2df) (MP2/6-311G(2df)) zero-point vibrational energy corrections were scaled by 0.9806 (0.9748).¹⁹ The calculations were performed using the electronic structure codes GAMESS,²⁰ Gaussian 03,²¹ and ACES II.²² The second derivatives were analyzed using the program BMATRIX.²³

Results and Discussion

Chemical Synthesis

In the synthesis of N_5^+ ,^{1,2} N_2F^+ was reacted with HN_3 to replace the F atom by an azido group (Eq. 1).



A similar approach was applied to the well known NOF_2^+ cation^{7,24-29} and, when a stoichiometric amount of HN_3 was used, formation of the N_3NOF^+ cation resulted (Eq. 2).

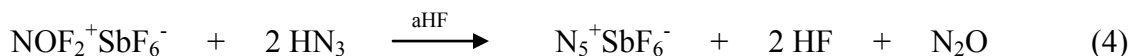


The $\text{N}_3\text{NOF}^+\text{SbF}_6^-$ salt was found to be marginally stable at ambient temperature³ and, therefore, an obvious challenge was to explore whether the second F atom could also be replaced by an azido group and, thus, provide a synthesis for the novel N_7O^+ cation (Eq. 3).



Replacement of F by N_3 started to proceed at temperatures as low as $-64\text{ }^\circ\text{C}$ and, when stoichiometric amounts of $\text{NOF}_2^+\text{SbF}_6^-$ and HN_3 were used, $\text{N}_3\text{NOF}^+\text{SbF}_6^-$ was formed in high yield and could be isolated by pumping off the solvent and gaseous products at low temperature. With an excess of HN_3 , replacement of the second fluorine atom started to occur in the same temperature range, however, the expected N_7O^+ cation could neither be directly observed by low-temperature NMR spectroscopy nor be

isolated in the form of its SbF_6^- salt. Instead, N_2O gas evolution and quantitative formation of $\text{N}_5^+\text{SbF}_6^{2-}$ was observed (Eq. 4).

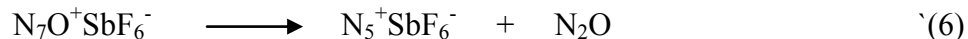


Since the $\text{NOF}_2^+\text{SbF}_6^-$ is more readily accessible⁸ than $\text{N}_2\text{F}^+\text{SbF}_6^-$, reaction (4) represents a more convenient and novel synthesis of $\text{N}_5^+\text{SbF}_6^-$.

Equations (2) - (4) represent an oversimplification of all the processes occurring in the $\text{NOF}_2^+/\text{HN}_3/\text{HF}$ system. NMR studies provided evidence for the presence and active participation of several equilibria. For example, at temperatures below -43°C in HF solution, HN_3 can displace NOF_3 from its $\text{NOF}_2^+\text{SbF}_6^-$ salt due to the fact that $\text{H}_2\text{N}_3^+\text{SbF}_6^-$ is practically insoluble in HF at low temperature (Eq. 5).



At -43°C , the NOF_3 is being consumed and N_3NOF^+ is formed. It is not clear whether the NOF_3 or NOF_2^+ is the reacting species, but generally NOF_2^+ is much more reactive than NOF_3 .^{7,24-29} At this temperature, N_3NOF^+ does not appear to react to an appreciable extent with HN_3 which, in the HF solution, is present in its protonated form, $\text{H}_2\text{N}_3^+\text{HF}_2^-(\text{nHF})$. When the temperature is raised to -33°C , the second mole of HN_3 starts to enter the reaction, all the NOF_3 is consumed and N_5^+ and N_2O are formed. Although ^{15}N labeling experiments (see below) show that the N_5^+ originates from an intermediate N_7O^+ , the N_7O^+ is not observable in the NMR spectra, indicating that its decomposition to N_5^+ and N_2O (Eq. 6) is more rapid than its formation.



It should be pointed out that protonated HN_3 in HF solution, i.e., $\text{H}_2\text{N}_3^+\text{HF}_2^-(\text{nHF})$, is less reactive towards NOF_2^+ than is HN_3 , requiring several days at room temperature to form N_3NOF^+ , N_5^+ and N_2O . This is not surprising because, due to their positive charges, the two cations should repel each other and not come in close enough contact for entering a reaction. The only reaction taking place would be through their equilibria with the neutral species.

Variation of the solvent (use of $(\text{CF}_3)_2\text{CFH}$) or the azide source (use of $(\text{CH}_3)_3\text{SiN}_3$) did not influence the outcome of these reactions. Obviously, the thermal stability of N_7O^+ must be significantly lower than that of N_3NOF^+ , thus preempting its direct observation and isolation. Because the N_7O^+ cation could not be directly observed, a theoretical study was carried out and its conclusions were experimentally corroborated by isotopic labeling experiments.

Theoretical Studies

Based on the known structure of $\text{N}_3\text{NOF}^{+3}$ and the reaction leading to its formation, the most probable structure for N_7O^+ , is the C_{2v} structure shown in Figure 1.

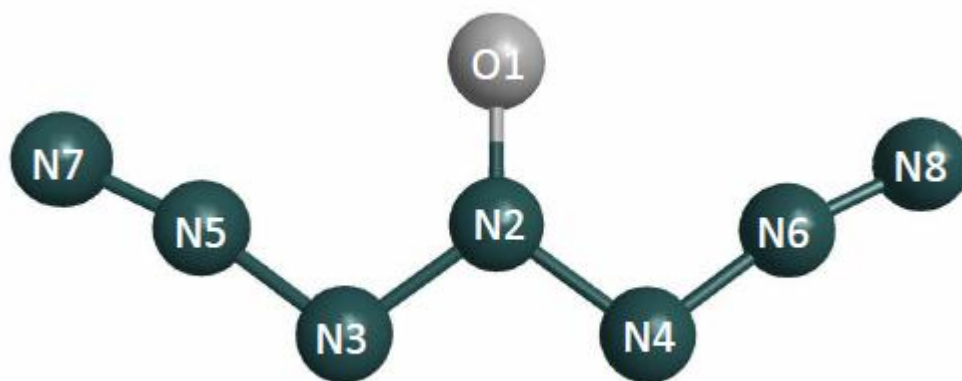


Figure 1. Minimum energy structure (bond distances in Å, angles in deg) of the C_{2v} isomer of N_7O^+ calculated at the MP2/cc-pvtz level with CCSD(T)/6-31G(d) values given in parentheses: O1-N2, 1.216 (1.221); N2-N3, 1.353 (1.371); N3-N5, 1.293 (1.320); N5-N7, 1.130 (1.131); O1-N2-N3, 126.2 (126.3); N2-N3-N5, 107.7 (106.9); N3-N5-N7, 170.6 (168.8); N2-N3-N5-N7, 180.0 (180.0). Weinhold's NBO charges at the PBE1PBE/6-311+G(2df) level: O -0.25; N2 0.46; N3 -0.13; N5 0.23; N7 0.29.

This structure was confirmed as the energy minimum by theoretical calculations at the B3LYP/6-311G(2df), MP2/6-311G(2df), MP2/cc-pvtz, and CCSD(T)/6-31G(d) levels of theory. Other possible

isomers have C_s and C_2 symmetry and a cyclic C_s structure (Fig. 2) and are higher in energy than the C_{2v} structure by 2.6, 17.8 and 27.8 kcal/mol, respectively, at the B3LYP/6-311G(2df) level of theory. The relatively small energy difference of 3 kcal/mol between the C_{2v} and C_s structures shows that the N_3 arm in N_7O^+ is quite floppy and can very easily be rotated, an important aspect to remember when potential mechanisms for the N_2O elimination from N_7O^+ are discussed.

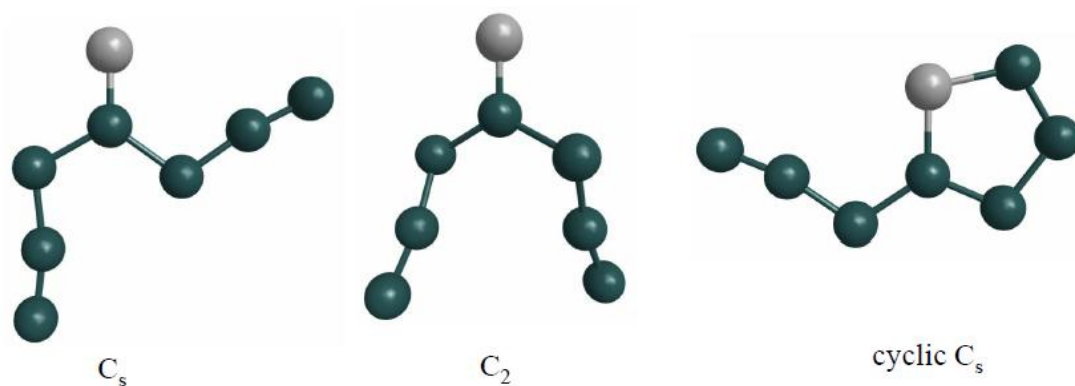


Figure 2. Higher energy, local minima structures for N_7O^+ . Oxygen (nitrogen) atoms are shown as light (dark) circles.

The calculated vibrational frequencies and infrared and Raman intensities are summarized in Table 1. As can be seen from the Table, the calculated frequencies are somewhat method dependent. Since in a catenated species consisting of several nearly linear groups of atoms with identical or similar masses, strong coupling of the vibrational modes must be expected, a normal coordinate analysis was also carried out for N_7O^+ at the B3LYP level. The results from this NCA are summarized in Table 2. The potential energy distribution shows that in most cases the normal vibrations are not highly characteristic and contain contributions from several symmetry coordinates, making many mode descriptions difficult, however, some assignments can be made. The dominant Raman mode, ν_1 , at 2314 cm^{-1} and the strong

Table 1 Harmonic vibrational frequencies (cm^{-1}), infrared intensities (km/mol), and Raman intensities [$\text{\AA}^4/\text{amu}$] of $\text{C}_{2v}\text{N}_7\text{O}^+$

	B3LYP(5)/cc-pvtz	MP2/cc-pvtz	CCSD(T)/6-31G(d)
$a_1 \quad v_1$	2314 (12) [460]	2194 (9.3) [529]	2234 (6.2)
v_2	1559 (153) [14]	1630 (85) [31]	1574 (104)
v_3	1176 (0.4) [12]	1194 (4.7) [29]	1110 (0.3)
v_4	968 (3.7) [7.6]	995 (1.6) [16.0]	969 (0.3)
v_5	525 (2.5) [13]	543 (1.0) [17]	503 (3.6)
v_6	427 (1.9) [2.3]	431 (1.8) [2.0]	411 (0.8)
v_7	134 (0.01) [6.7]	131 (0.02) [8.3]	129 (0.1)
$a_2 \quad v_8$	504 (0) [2.0]	475 (0) [1.2]	452 (0)
v_9	166 (0) [0.2]	161 (0) [0.005]	140 (0)
$b_1 \quad v_{10}$	703 (9.3) [0.15]	712 (6.3) [0.3]	687 (10)
v_{11}	540 (6.1) [0.02]	511 (4.1) [0.04]	498 (4.8)
v_{12}	94 (1.0) [0.08]	97 (1.1) [0.04]	93 (1.8)
$b_2 \quad v_{13}$	2307 (276) [40]	2182 (383) [61]	2222 (288)
v_{14}	1220 (1069) [3.1]	1323 (1431) [5.9]	1219 (1281)
v_{15}	1008 (70) [0.1]	1015 (116) [2.7]	933 (220)
v_{16}	798 (10) [1.2]	835 (7.4) [1.8]	794 (43)
v_{17}	495 (0.1) [0.02]	501 (1.4)[0.06]	478 (0.03)
v_{18}	225 (2.8) [1.5]	221 (1.6) [0.6]	215 (2.8)

IR mode, v_{13} , at 2307 cm^{-1} are predominantly due to the in-phase and out-of-phase coupled stretching modes, respectively, of the two terminal N-N bonds. The 1559 cm^{-1} vibration, v_2 , is 51 % stretching of the N-O bond, and the dominant infrared mode, v_{14} , at 1220 cm^{-1} is 60 % due to the rocking motion of

Table 2 B3LYP/cc-pvtz Force Constants^a and Potential Energy Distribution^b of C_{2v} N₇O⁺

Symmetry Class	Frequency cm ⁻¹	Force Constants							PED
		F ₁₁	F ₂₂	F ₃₃	F ₄₄	F ₅₅	F ₆₆	F ₇₇	
a ₁	2314	21.351	0.182	1.260	-0.478	-0.098	-0.209	0.102	75.1S ₁ + 23.8S ₃
	1559		11.249	-0.280	1.674	1.090	0.061	0.019	51.4S ₂ + 18.7S ₆ + 15.5S ₄ + 13.4S ₅
	1176			7.078	0.558	-0.650	1.121	0.261	61.3S ₃ + 23.0S ₄
	968				6.048	-1.001	0.881	-0.009	44.9S ₆ + 26.4S ₇ + 14.2S ₄
	525					4.076	-0.275	-0.037	86.6S ₇
	427						1.710	0.083	79.7S ₇ + 16.7S ₅
	133							0.425	66.9S ₇ + 28.3S ₆
a ₂	504	F ₈₈	F ₉₉						98.5S ₉
	166	0.125	-0.001						76.4S ₁₂ + 23.5S ₁₁
b ₁	703	F _{10,10}	F _{11,11}	F _{12,12}					55.4S ₁₁ + 44.7S ₁₀
	540	0.785	-0.298	-0.014					99.1S ₁₂
	94		0.278	0.009					76.4S ₁₂ + 23.5S ₁₁
b ₂	2307	F _{13,13}	F _{14,14}	F _{15,15}	F _{16,16}	F _{17,17}	F _{18,18}		75.3S ₁₃ + 22.8S ₁₄
	1220	21.336	1.321	-0.504	-0.186	-0.003	0.106		60.1S ₁₇ + 28.3S ₁₅
	1008		6.703	0.715	1.017	-0.271	0.273		82.0S ₁₄ + 10.5S ₁₇
	798			4.446	0.852	0.451	-0.022		43.1S ₁₈ + 36.6S ₁₆ + 10.6S ₁₇
	495				1.593	0.060	0.069		67.8S ₁₈ + 24.8S ₁₇
						1.395	-0.005		76.9S ₁₈ + 19.1S ₁₆
	225						0.419		

^a Stretching constants in mdyne/Å, deformation constants in mdyne-Å/rad², and stretch-bend interaction constants in mdyne/rad.

^b PED in percent. Coordinates contributing less than 10 percent have been omitted. Coordinates have been defined as follows (normalization factors have been omitted): S₁ = ν(N₅-N₇)+ν(N₆-N₈), S₂ = ν(O-N₂), S₃ = ν(N₃-N₅)+ν(N₄-N₆), S₄ = ν(N₂-N₃)+ν(N₂-N₄), S₅ = δ(O-N₂-N₃)+δ(O-N₂-N₄), S₆ = δ(N₂-N₃-N₅)+δ(N₂-N₄-N₆), S₇ = δ(N₃-N₅-N₇)+δ(N₄-N₆-N₈), S₈ = ω(O-N₂-N₃-N₅)+ω(O-N₂-N₄-N₆), S₉ = ω(N₂-N₃-N₅-N₇)+ω(N₂-N₄-N₆-N₈), S₁₀ = ω(O-N₂-N₃-N₄), S₁₁ = ω(O-N₂-N₃-N₅)-ω(O-N₂-N₄-N₆), S₁₂ = ω(N₂-N₃-N₅-N₇)-ω(N₂-N₄-N₆-N₈), S₁₃ = ν(N₅-N₇)-ν(N₆-N₈), S₁₄ = ν(N₃-N₅)-ν(N₄-N₆), S₁₅ = ν(N₂-N₃)-ν(N₂-N₄), S₁₆ = δ(N₂-N₃-N₅)-δ(N₂-N₄-N₆), S₁₇ = δ(O-N₂-N₃)-δ(O-N₂-N₄), S₁₈ = δ(N₃-N₅-N₇)-δ(N₄-N₆-N₈)

the oxygen atom. The isotopic shifts which should be observed in the vibrational spectra upon replacement of ^{16}O by ^{18}O and of all ^{14}Ns by ^{15}Ns have also been calculated. The results are summarized in Table 3.

Table 3 ^{18}O and ^{15}N Isotopic Shifts (cm^{-1}) of $\text{C}_{2v} \text{N}_7\text{O}^+$ at the B3LYP/cc-pvtz level

$^{16}\text{O}-^{14}\text{N}$	$^{18}\text{O}-^{14}\text{N}$	$^{16}\text{O}-^{15}\text{N}$	$^{18}\text{O}-^{15}\text{N}$	$(^{18}\text{O}-^{14}\text{N}) - (^{16}\text{O}-^{14}\text{N})$	$(^{16}\text{O}-^{15}\text{N}) - (^{16}\text{O}-^{14}\text{N})$	$(^{18}\text{O}-^{15}\text{N}) - (^{16}\text{O}-^{14}\text{N})$
2314.0	2314.0	2235.6	2235.6	0.0	-78.4	-78.4
2307.7	2307.7	2229.5	2229.5	0.0	-78.2	-78.2
1558.9	1525.9	1526.9	1492.3	-33.0	-32.0	-66.6
1220.2	1218.2	1180.1	1178.0	-2.0	-40.1	-42.2
1176.2	1175.2	1136.9	1135.9	-1.0	-39.3	-40.3
1007.9	1007.4	974.0	973.5	-0.5	-33.9	-34.4
968.0	955.1	942.2	930.1	-12.9	-25.8	-37.9
798.1	795.4	772.7	769.9	-2.7	-25.4	-28.2
703.2	698.9	682.0	677.6	-4.3	-21.2	-25.6
539.6	539.5	521.3	521.2	-0.1	-18.3	-18.4
525.2	524.7	507.8	507.2	-0.5	-17.4	-18.0
504.5	504.5	487.4	487.4	0.0	-17.1	-17.1
494.9	483.7	484.8	473.5	-11.2	-10.1	-21.4
427.4	424.0	414.7	411.6	-3.4	-12.7	-15.8
225.3	221.1	220.1	216.0	-4.2	-5.2	-9.3
166.4	166.4	160.8	160.8	0.0	-5.6	-5.6
133.9	133.1	129.7	129.0	-0.8	-4.2	-4.9
93.7	92.3	91.4	90.0	-1.4	-2.3	-3.7

Finally, the nitrogen NMR shifts have also been calculated for N_7O^+ at the PBE1BPE/6-311+G(2df) level of theory. The following chemical shifts in ppm relative to CH_3NO_2 are predicted: $\text{N}_2 = -10.2$, $\text{N}_3 = -157.9$, $\text{N}_5 = -164.0$, $\text{N}_7 = -64.8$. These data will facilitate future experimental searches for this interesting cation.

Since all attempts to isolate N_7O^+ had been unsuccessful, while N_3NOF^+ possesses good thermal stability, the question arose whether this was due to a poor choice of reagents or reaction conditions or if there is a general innate stability problem with geminal di-azides. In order to deal with this problem, it is imperative to understand the decomposition mechanism of N_7O^+ and *gem*-di-azides in general.

In the study of the decomposition of N_7O^+ , five different pathways were found with transition states (TS), which are illustrated in Figure 3 and with relative energies summarized in Figure 4. Intrinsic reaction coordinate (IRC) calculations were performed to trace the minimum energy pathway from each transition state to reactants and products. Two of the five transition states originate from the C_{2v} ground state and involve the interaction of the negatively charged oxygen atom with either a positively charged $\text{N}\beta$ atom of an azido group, resulting in a four-membered ring (TS 1), or an also positively charged $\text{N}\gamma$ atom resulting in a five-membered ring (TS 2). (The NBO charge distributions of N_7O^+ are given in the diagram caption of Figure 1.) Note that in case of TS 2, the decomposition pathway is actually a two-step process that goes through a cyclic intermediate I2, which is the same as the cyclic structure shown in Figure 2. The transition state structures preceding (TS2a) and following (TS2b) formation of I2 are nearly identical in structure and relative energy, and therefore only TS2b is shown in Figure 3.

Since the energy difference between the C_{2v} and the C_s structure is only ~ 3 kcal/mol with a low interconversion barrier of ~ 14 kcal/mol, a possible decomposition mechanism starting from the C_s state was also explored. Again, there can be an interaction between the O atom with either $\text{N}\beta$ (TS 4) or $\text{N}\gamma$ (TS 5) of that azido group which points in the same direction as the oxygen. Similar to

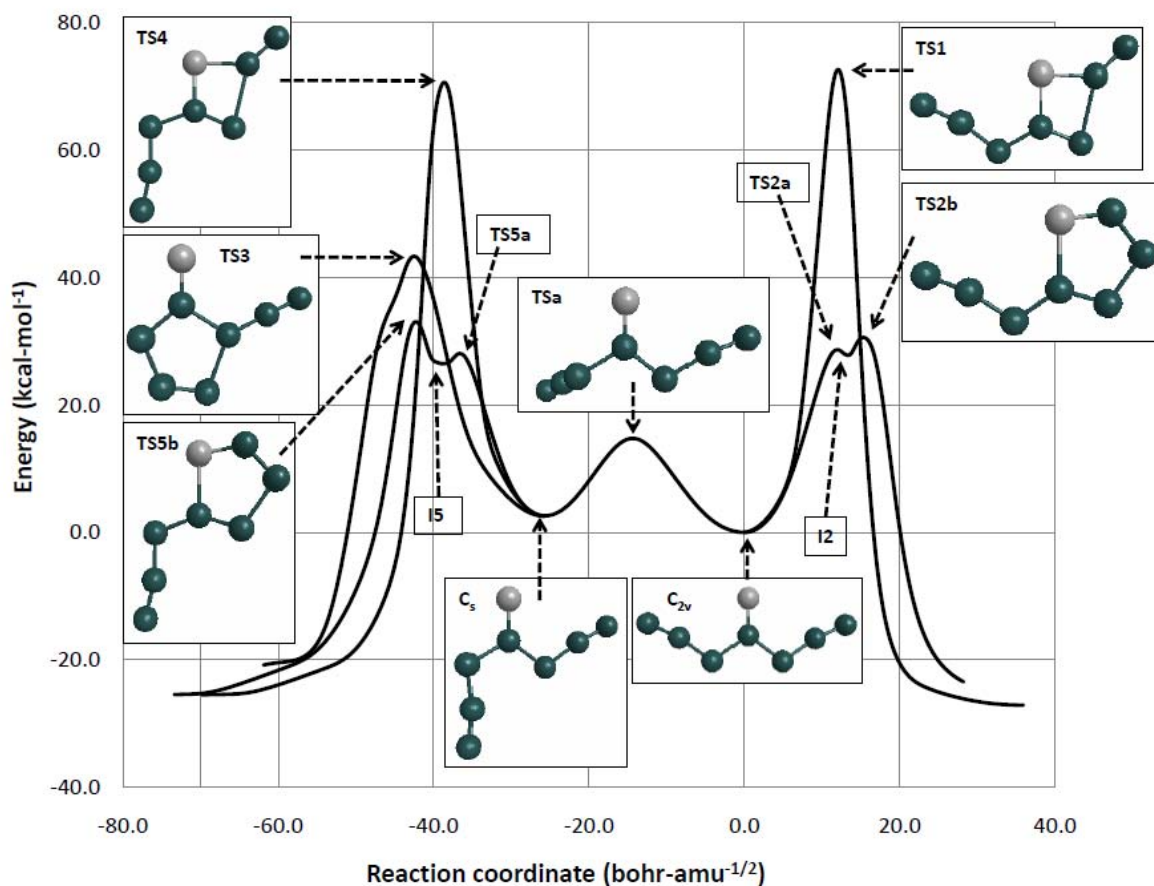


Figure 3. B3LYP/6-311G(2df) intrinsic reaction coordinate traces (solid curves) and stationary points for the decomposition reaction of N_7O^+ . Oxygen (nitrogen) atoms are shown as light (dark) circles. Local minimum I2 is identical to the cyclic isomer shown in Figure 2.

the TS 2 reaction pathway discussed previously, the TS 5 decomposition pathway is actually a two-step process going through a cyclic intermediate I5, preceded and followed by TS5a and TS5b, respectively. The TS5a, TS5b, and I5 stationary points are nearly identical in structure and relative energy, and therefore only TS5b is illustrated in Figure 3. An additional decomposition pathway involves the interaction between the positively charged N_γ atom of the azido group pointing away from the oxygen atom with the negatively charged N_α atom of the azido group pointing in the same direction as the oxygen atom (TS 3). The calculated barriers are shown in Figures 3 and 4. As can be seen, the barriers involving four-membered cyclic transition states are ~ 70 kcal/mol and are much higher than those involving five-membered rings and, therefore, can be discounted.

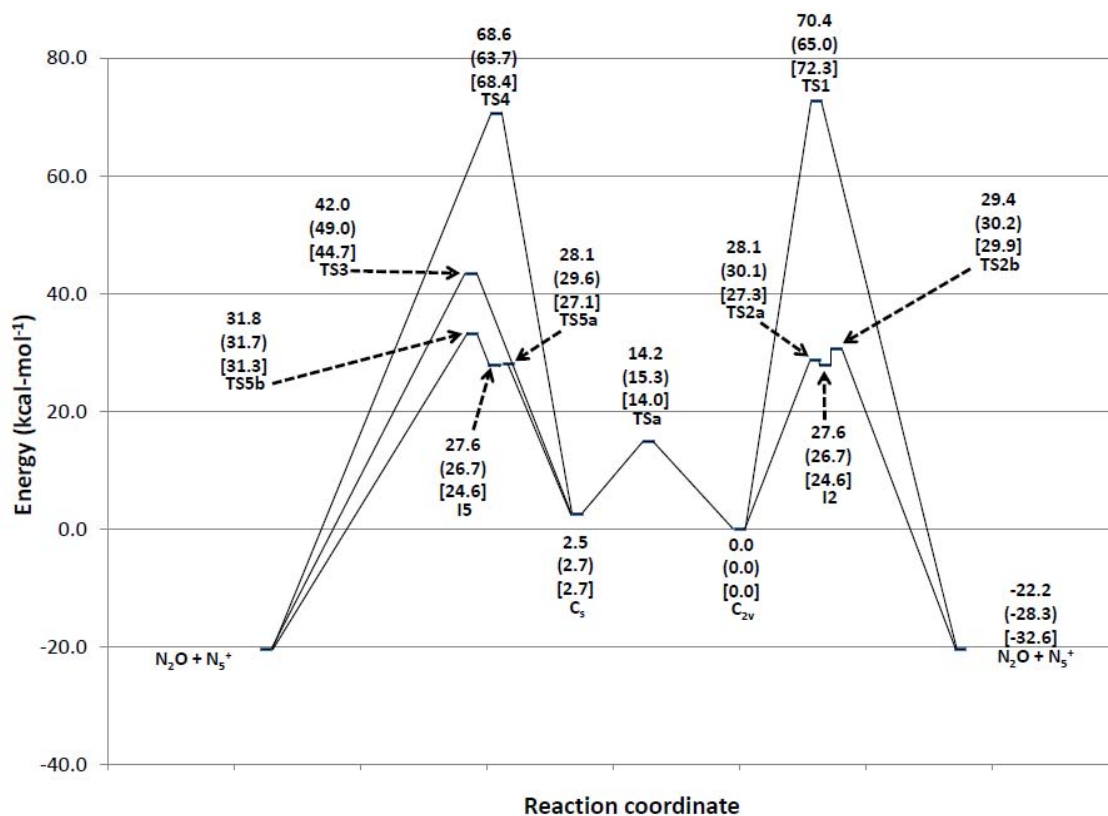
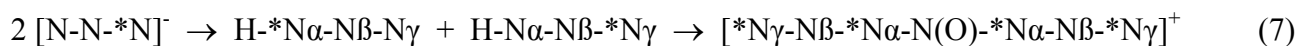


Figure 4. Relative energies (kcal/mol), at the B3LYP/6-311G(2df) level of theory, including scaled B3LYP zero point vibrational energy corrections. MP2/6-311G(2df) and CR-CCSD(T)/cc-pvtz//MP2/6-311G(2df) values, both of which include scaled MP2 zero point vibrational energies, are shown in parentheses and brackets, respectively.

To further discriminate between the different decomposition mechanisms, decomposition studies have been carried out using ¹⁵N labels. For this purpose, labeled N₇O⁺ with partial ¹⁵N labels in the N α and the N γ positions were prepared, using singly, terminally labeled azide ion as the starting material (Eq. 7).



The distribution of the ¹⁵N labels in the N₇O⁺ decomposition products was determined by ¹⁵N NMR spectroscopy. It was found that the N₂O was exclusively labeled on the terminal N, i.e., ^{*}N-N-O, and that in N₅⁺ the ¹⁵N label was equally distributed over all five positions. Of the five different mechanisms that were studied, only the mechanism TS 3 involving the attack of the positively charged N γ atom of

the azido group pointing away from the oxygen atom on the negatively charged N α atom of the azido group pointing in the same direction as the oxygen atom can account for the observed distribution of the ^{15}N labels (Fig. 5) and has a reasonably low activation barrier (~ 42 kcal/mol) which is about half

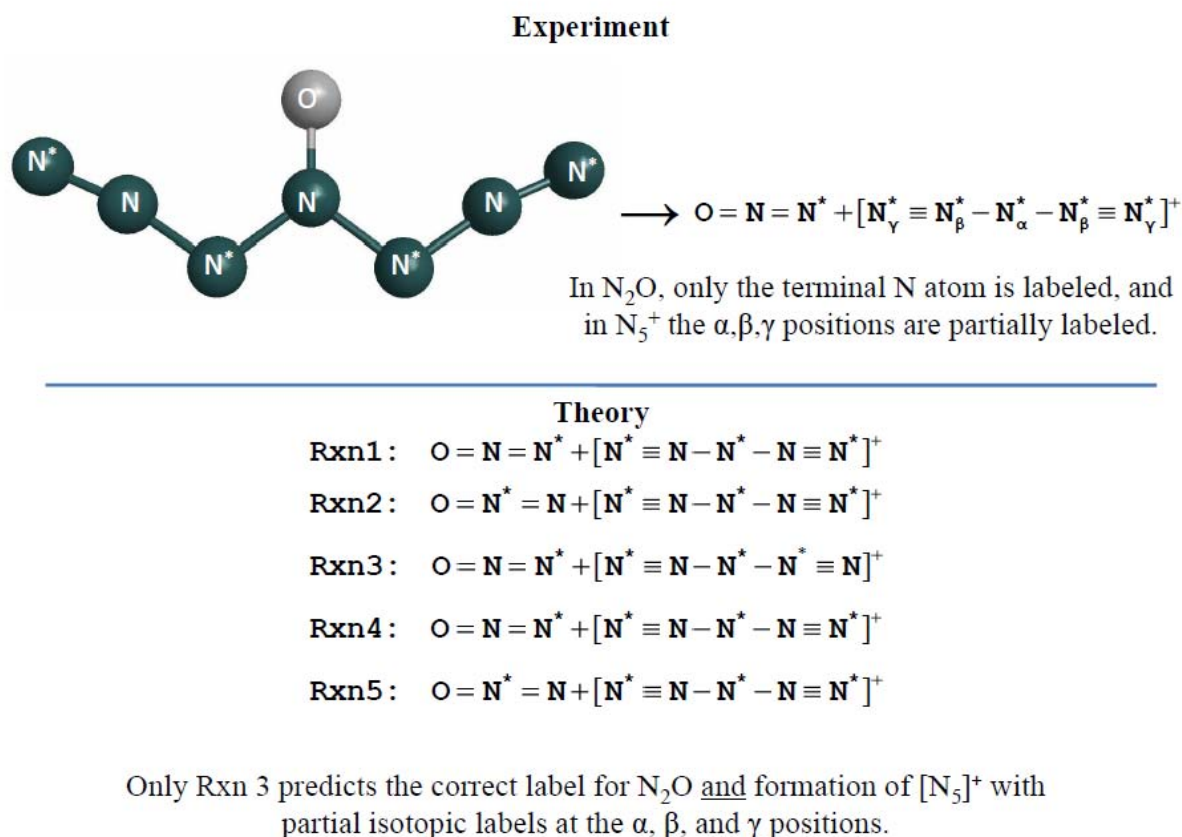


Figure 5. Comparison of the theoretically predicted and the experimentally found ^{15}N labels in the decomposition products of N_7O^+ .

of that predicted for N_3NOF^+ (~ 80 kcal/mol). Although all of these barriers are higher than expected, it is possible that the calculations overestimate the size of the barriers and/or that the barriers in solution are considerably lower than in the free gas phase. Nevertheless, this study clearly demonstrates that the di-azido N_7O^+ cation has a much lower barrier than the mono-azido N_3NOF^+ cation, in excellent agreement with the experimental observations. Furthermore, the fact that the preferred mechanism requires the presence of two geminal azido ligands explains the general observation in azide chemistry

that geminal diazides are much more sensitive and unstable than either mono-azides or vicinal di-azides. The inadvertent formation of geminal di-azides as a by product in the synthesis of mono-azides has led in the past to severe accidents and injuries and must be avoided under all circumstances. These conditions apply not only to azide substituted amine oxides, but are equally valid for azidamines and other similar compounds, the only difference being the nature of the elimination product. In the case of multiply azide substituted amines, the elimination product becomes N_2 instead of N_2O , but the decomposition mechanism remains the same.

Conclusions

The N_7O^+ cation was prepared from the low-temperature reaction of NOF_2^+ with a twofold excess of HN_3 in anhydrous HF solution. The N_7O^+ cation is thermally very unstable and decomposes instantaneously to N_5^+ and N_2O , thus preventing its direct observation. However, its formation was well established by NMR spectroscopy of the decomposition products, by the use of ^{15}N labeling and by the results from a theoretical study. The decomposition mechanism of N_7O^+ was analyzed and involves the electrophilic attack of the terminal gamma-N atom of one azide ligand on the electron rich alpha-N atom of the second azide ligand, thus explaining the generally observed instability of geminal di-azides.

Acknowledgements

This work was funded by the Air Force Office of Scientific Research, the Office of Naval Research, the Defense Threat Reduction Agency, and the National Science Foundation. Any opinions, findings, and conclusions or recommendations expressed in this material are those of the authors and do not necessarily reflect the views of the National Science Foundation.

References

- (1) Christe, K. O., Wilson, W. W., Sheehy, J. A., Boatz, J. A., *Angew. Chem. Int. Ed.* **1999**, *38*, 2004.
- (2) Vij, A., Wilson, W. W., Vij, V., Tham, F. S., Sheehy, J. A., Christe, K. O., *J. Am. Chem. Soc.* **2001**, *123*, 6308.
- (3) Wilson, W. W., Haiges, R., Boatz, J. A., Christe, K. O., *Angew. Chem. Int. Ed.* **2007**, *46*, 3023.
- (4) Vij, A., Pavlovich, J. G., Wilson, W. W., Vij, V., Christe, K. O., *Angew. Chem. Int. Ed.* **2002**, *41*, 3051.
- (5) Christe, K. O., *Prop., Explos., Pyrotech.* **2007**, *32*, 194.
- (6) Christe, K. O., Wilson, W. W., Schack, C. J., Wilson, R. D., *Inorg. Synth.* **1986**, *24*, 39.
- (7) Christe, K. O., *J. Am. Chem. Soc.* **1995**, *117*, 6136.
- (8) Christe, K. O., Wilson, W. W., Schack, C. J., *J. Fluorine. Chem.* **1978**, *11*, 71.
- (9) Moller, C., Plesset, M. S., *Phys. Rev.* **1934**, *46*, 618; Pople, J. A., Binkley, J. S., Seeger, R., *Int. J. Quantum Chem.* **1976**, *S10*, 1; Frisch, M. J., Head-Gordon, M., Pople, J. A., *Chem. Phys. Lett.* **1990**, *166*, 275; Bartlett, J., Silver, D. M., *Int. J. Quantum Chem. Symp.* **1975**, *9*, 1927.
- (10) Krishnan, R., Binkley, J. S., Seeger, Pople, J. A., *J. Chem. Phys.* **1980**, *72*, 650; Frisch, M. J., Pople, J. A., Binkley, J. S., *J. Chem. Phys.* **1984**, *80*, 3265.
- (11) Dunning, Jr. T. H., *J. Chem. Phys.* **1989**, *90*, 1007.
- (12) Becke, A. D., *J. Chem. Phys.* **1993**, *98*, 5648; Stephens, P. J., Devlin, F. J., Chablowski, C. F., Frisch, M. J., *J. Phys. Chem.* **1994**, *98*, 11623; Hertwig, R. H., Koch, W., *Chem. Phys. Lett.* **1997**, *268*, 345.
- (13) Vosko, S. H., Wilk, L., Nusair, M., *Can. J. Phys.* **1980**, *58*, 1200.

- (14) Purvis, G. D. III, Bartlett, R. J., *J. Chem. Phys.* **1982**, 76, 1910.
- (15) Hehre, W. J., Ditchfield, R., Pople, J. A., *J. Chem. Phys.* **1972**, 56, 2257; Hariharan, P. C., Pople, J. A., *Theoret.Chim.Acta* **1973**, 28, 213.
- (16) Ishida, K., Morokuma, K., Komornicki, A., *J. Chem. Phys.* **1977**, 66, 2153.
- (17) Gonzales, C., Schlegel, H. B., *J. Chem. Phys.* **1989**, 90, 2154.
- (18) Piecuch, P., Kucharski, S. A., Kowalski, K., Musial, M., *Comp. Phys. Commun.* **2002**, 149, 71; Kowalski, K., Piecuch, P., *J. Chem. Phys.* **2000**, 113, 18; Kowalski, K., Piecuch, P., *J. Chem. Phys.*, **2000**, 113, 5644.
- (19) Scott, A. P., Radom, L., *J. Phys. Chem.* **1996**, 100, 16502.
- (20) a) Schmidt, M. W., Baldridge, K. K., Boatz, J. A., Elbert, S. T., Gordon, M. S., Jensen, J. H., Koseki, S., Matsunaga, N., Nguyen, K. A., Su, S. J., Windus, T. L., Dupuis, M., Montgomery, J. A., *J. Comput. Chem.* **1993**, 14, 1347; b) Gordon, M. S., Schmidt, M. W.; pp. 1167-1189, in "Theory and Applications of Computational Chemistry: the first forty years" C.E.Dykstra, G.Frenking, K.S.Kim, G.E.Scuseria (editors), Elsevier, Amsterdam, 2005.
- (21) Gaussian 03, Revision D.01, M. J. Frisch, G. W. Trucks, H. B. Schlegel, G. E. Scuseria, M. A. Robb, J. R. Cheeseman, J. A. Montgomery, Jr., T. Vreven, K. N. Kudin, J. C. Burant, J. M. Millam, S. S. Iyengar, J. Tomasi, V. Barone, B. Mennucci, M. Cossi, G. Scalmani, N. Rega, G. A. Petersson, H. Nakatsuji, M. Hada, M. Ehara, K. Toyota, R. Fukuda, J. Hasegawa, M. Ishida, T. Nakajima, Y. Honda, O. Kitao, H. Nakai, M. Klene, X. Li, J. E. Knox, H. P. Hratchian, J. B. Cross, V. Bakken, C. Adamo, J. Jaramillo, R. Gomperts, R. E. Stratmann, O. Yazyev, A. J. Austin, R. Cammi, C. Pomelli, J. W. Ochterski, P. Y. Ayala, K. Morokuma, G. A. Voth, P. Salvador, J. J. Dannenberg, V. G. Zakrzewski, S. Dapprich, A. D. Daniels, M. C. Strain, O. Farkas, D. K. Malick, A. D. Rabuck, K. Raghavachari, J. B. Foresman, J. V. Ortiz, Q. Cui, A. G. Baboul, S. Clifford, J. Cioslowski, B. B. Stefanov, G. Liu, A. Liashenko, P. Piskorz, I. Komaromi, R. L. Martin, D. J. Fox, T. Keith, M. A. Al-Laham, C. Y. Peng, A.

Nanayakkara, M. Challacombe, P. M. W. Gill, B. Johnson, W. Chen, M. W. Wong, C. Gonzalez, and J. A. Pople, Gaussian, Inc., Wallingford CT, 2004.

(22) Stanton, J. F., Gauss, J., Watts, J. D., Nooijen, M., Oliphant, N., Perera, S. A., Szalay, P. G., Lauderdale, W. J., Gwaltney, S. R., Beck, S., Balkova, A., Bernholdt, D. E., Baeck, K. K., Rozyczko, P., Sekino, H., Hober, C., Bartlett, R. J., *ACES II, Quantum Theory Project*; University of Florida: Integral packages included are VMOL (Almlof, J., Taylor, P. R.), BPROPS (Taylor, P. R.), and ABACUS (Helgaker, T., Jensen, H. J. Aa, Jorgensen, P., Olsen, J., Taylor, P. R.).

(23) Komornicki, A., *BMATRIX Version 2.0*; Polyatomics Research Institute: Palo Alto, CA, **1996**.

(24) Fox, W. B., MacKenzie, J. S., Vanderkooi, N., Sukorkik, B., Wamser, C. A., Holmes, J. R., Eibeck, R. E., Stewart, B. B., *J. Am. Chem. Soc.* **1966**, 88, 2604.

(25) Christe, K. O., Maya, W., *Inorg. Chem.* **1969**, 8, 1253.

(26) Wamser, C. A., Fox, W. B., Sukornik, B., Holmes, J. R., Stewart, B. B., Juurick, R., Vanderkooi, N., Gould, D., *Inorg. Chem.* **1969**, 8, 1249.

(27) Christe, K. O., Hon, J. F., Pilipovich, D., *Inorg. Chem.* **1973**, 12, 84.

(28) Mason, J., Christe, K. O., *Inorg. Chem.* **1983**, 22, 1849.

(29) Vij, A., Zhang, X., Christe, K. O., *Inorg. Chem.* **2001**, 40, 416.

Synopsis

The reaction of NOF_2^+ with two moles of HN_3 produces the novel N_7O^+ cation which rapidly decomposes to N_5^+ and N_2O in a quantitative manner. Isotopic labeling elucidates the decomposition mechanism of N_7O^+ and explains why geminal di-azides are much less stable than either mono-azides or geminal di-azides.

Synopsis Artwork

